Mining Science, vol. 33, 2026, 7–24

www.miningscience.pwr.edu.pl

Mining Science

(Previously Prace Naukowe Instytutu Gornictwa Politechniki Wroclawskiej, ISSN 0370-0798)

ISSN 2300-9586 (print)
ISSN 2353-5423 (online)

Received June 17, 2025; Reviewed; Accepted January 30, 2026

QUANTITATIVE DISCHARGE MODEL OF A SINGLE-SIDED PLOW-TYPE DISCHARGER

Yingxin XIE, Mingxu WANG*,
Zhongqi HE， Mengfei LIU

[1] Henan University of Technology, Zhengzhou, Henan, China

Abstract: Current gob filling devices are mostly bottom-dump scraper conveyors. Due to the structural characteristics of the scraper, the scraper-type Backfilling Slinger has high working noise, high energy consumption, and low conveying efficiency. In response to the above issues, this paper proposes the structural design of a belt-type gob Backfilling Slinger and suggests using a single-sided plow-type unloader for unloading. This paper models the unloading process mathematically, providing two types of unloading models: one that follows the angle of repose for stacking and the other that spreads evenly in the middle section. Subsequently, an experimental platform is used for unloading experiments to verify the correctness of the model. Finally, by comparing the casting performance of scraper-type and belt-type machines, it is found that, without considering the service life, the unloading capacity of the belt-type gob Backfilling Slinger has increased by about 75% compared to the scraper conveyor.

***Keywords*:** *gob Backfilling Slinger, plow-type unloader, unloading model*

1. INTRODUCTION

Coal gangue is a solid waste in coal mining operations, accounting for about 10%–25% of the total coal production, and its large accumulation will cause serious damage to the surrounding. Coal has a long history of use and is currently a major source of energy. In the process of coal mining, a huge amount of coal gangue that cannot be digested in
a large scale is generated. Taking China as an example, the annual output of coal

* Corresponding author: wmx20032002@163.com (M. Wang)

doi: 10.37190/msc/217636

gangue is about 800 million tons, but its utilization rate is only about 70% (Cui et al. 2025; Huang 2012). However, the local storage not only occupies land but also poses environmental pollution risks. At present, about 20% of coal gangue is used for backfilling of mining pits. With the increase of coal mining, the demand for the transportation of coal gangue is getting higher and higher. Quantitative unloading during backfilling can reduce the time consumed by uniform throwing within the radiation range, so the efficient quantitative throwing machine has become a key research direction.

At present, the form of the throwing machine is mostly the chain conveyor of the buried scraper type. Wu Yuyi (2024) proposed a comprehensive mining throwing gangue filling technology based on the form of the chain conveyor, which realizes the transportation of coal gangue by driving the scraper to rotate. Xuewen Wang (2018) carried out a numerical simulation on the transportation process of the scraper conveyor, and obtained the influencing factors of the chute stress and deformation, providing theoretical guidance for the optimization of the scraper machine structure. However, the friction between the material and each part of the scraper bottom unloading type throwing machine is relatively large during work, which leads to higher energy consumption of the whole machine and lower life of key parts. In addition, because its unloading method is to open a hole at the unloading position of the chain plate, and the material falls down through the opening to achieve unloading. Since the unloading amount of the same stacking form of material is different when the chain plate speed changes, this unloading method cannot accurately control the unloading amount of each unloading port. For Yin Rui, Zhang Dongxue, Ni Qiang (2024) the real-time simulation of the unit amount of coal of the scraper conveyor is realized through the multi-parameter mathematical modeling method, thereby intuitively reflecting the coal mining process in the mine and accurately calculating the real-time coal carrying amount of the scraper conveyor. Compared with the defects of the scraper conveyor, the large-output belt machine combined with the plow-type unloader can realize the large-output throwing of gangue. The research on the plow type is mostly concentrated on the simulation analysis, Paul W. Cleary (2013) used DEM to study the plow-type mixer and found that the more realistic representation of particle shape has a significant impact on the simulation of the bed strength and mixing efficiency. Yang Ning (2022) based on DEM research on the spillage, pollution and wear analysis of the plow-type unloader and proposed the plow-type unloader. Mingliang et al. (2022) based on DEM analysis of the impact wear and unloading average speed during the unloading process, obtained the optimal curvature radius. Yao Yan and Xiangyu Gu (2023) based on DEM research on the wear analysis of the plow-type unloader, obtained the optimal curvature radius.

Combining the above research, this paper designs a belt conveyor type of throwing machine, which realizes the control of the unloading amount by controlling the opening angle of the multi-level single-sided plow-type unloader. First, a mathematical model of the unloading of the throwing machine under different stacking forms is established,

and the relationship between the opening angle of the three-level guide plate and the unloading amount under different stacking forms is established. By analyzing whether the material stacking collapse caused by the first-level unloading angle affects the second-level unloading amount, the relationship between the unloading angle and the unloading amount of the three-level unloading port is determined. Finally, the verification experiment is carried out through the simulation and the three-level unloading throwing machine experimental platform built, and the maximum error between the results of multiple experiments and the two models does not exceed 10%, verifying the application scenarios of the two throwing models.

2. MATHEMATICAL MODEL OF UNLOADING OF BELT GANGUE THROWER

Coal gangue is a by-product generated during coal mining and processing. As shown in Fig. 1, the gangue first undergoes crushing and pre-treatment, followed by testing. High calorific value gangue is utilized for power generation, while low calorific value gangue is used for backfilling and producing building materials. Backfilling represents the primary application, accounting for approximately 42% of the total. In coal gangue backfilling, the Backfilling Slinger is the primary conveying equipment. Currently, scraper conveyors with bottom discharge are widely used; however, they suffer from short service life due to severe scraper friction during operation, and their limited backfilling range necessitates frequent relocation. To achieve high-efficiency backfilling, a high-capacity belt-type Backfilling Slinger is designed.

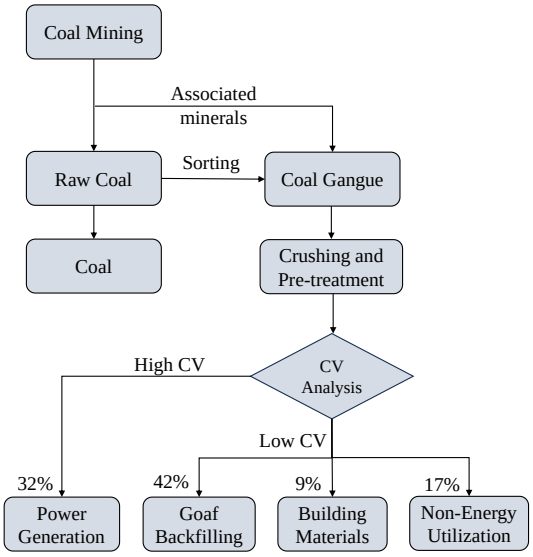

Fig. 1. Discharge process

The kinematic schematic of the designed experimental-scale belt-type Backfilling Slinger is shown in Fig. 2. It primarily consists of a feed hopper, a belt conveyor, and a single-sided plow discharger. By controlling the servo motor, the opening angle of the plow discharger can be adjusted to achieve quantitative unloading.

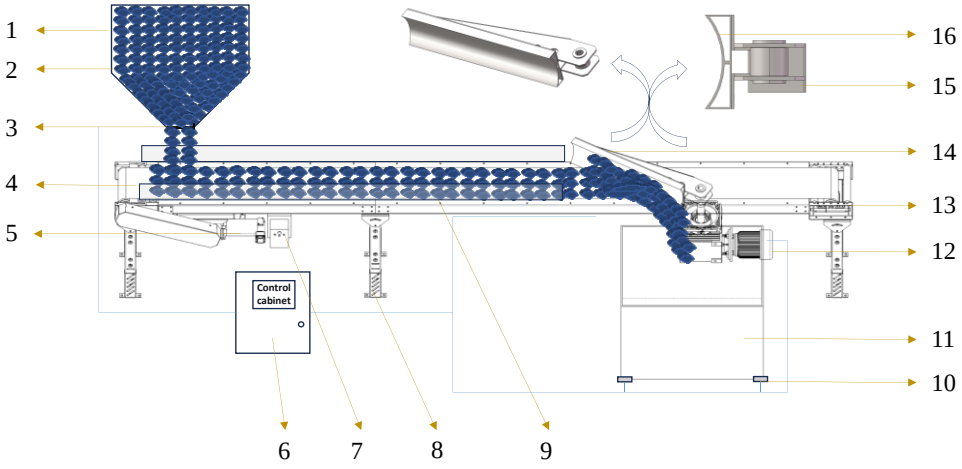

Fig. 2. Schematic diagram of the belt-type Backfilling Slinger:
1 – coal gangue, 2 – feed hopper, 3 – slide gate valve, 4 – conveyor belt, 5 – driver motor,
6 – control cabinet, 7 – frequency converter, 8 – frame, 9 – guide plate, 10 – load cell,
11 – collection bin, 12 – servo motor, 13 – tensioning device, 14 – single-sided plow unloader,
15 – fixed frame, 16 – deflector plate

2.1. ESTABLISHMENT OF THE UNLOAD MATHEMATICAL MODEL

When establishing the mathematical model, the material's stacking form and belt speed are key factors affecting the discharge amount. The material's movement and stacking angle will also change with different belt speeds. This paper takes into account the changes in the stacking angle of different materials at different belt speeds, and establishes the discharge mathematical model with the stacking angle and belt speed as known variables (Zhao 2020). The discharge process is shown in Fig. 3.

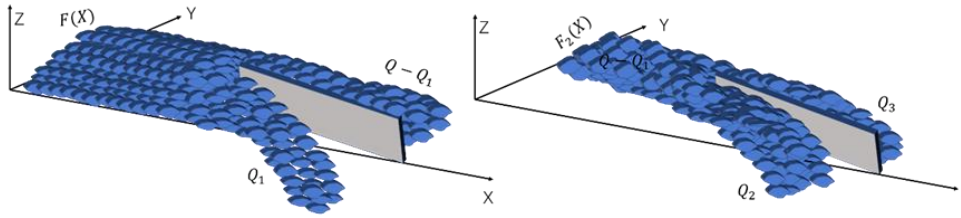

Fig. 3. Discharge process

2.2. FITTING THE MATERIAL CONTOUR TRAJECTORY WITH A PARABOLA

When the belt speed is known as v and the dynamic angle of repose of the material is γ, with the material pile height being h, the belt width B, and the length of the discharge plate L, the range of values for the discharge opening angle θ can be determined

$$0 \le \theta \le \arcsin\frac{B}{L}.$$

The parabolic approximation of the material contour stems directly from bulk material dynamics and practical engineering constraints. Continuous vibrations during high-speed operation induce material settling and "micro-slumping", rounding the sharp apex of the static pile into a smooth curved profile governed by the dynamic surcharge angle. This naturally formed geometry aligns closely with a parabolic shape, yielding a theoretical approximation error under typical loading conditions that is far below the measurement noise of on-site sensors. Furthermore, the simpler analytical form of the parabolic model eliminates complex trigonometric calculations, significantly enhancing the efficiency of cross-sectional integration and flow estimation to meet the rigorous demands of real-time quantitative control. Using a parabolic fit $F(X) = aX^2 + bX^2 + c$ to model the contour of the material interface.

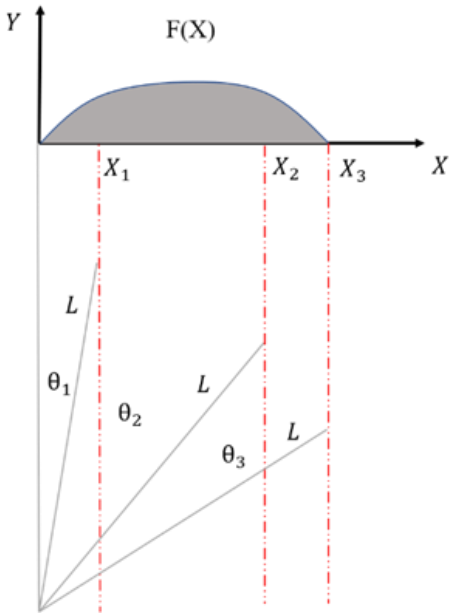

Fig. 4. Parabola fitting: ($F(X)$ – is the outline of material stacking interface, θ – is opening angle of plow unloader, X – is the horizontal coordinate corresponding to the θ angle)

From the above Fig. 4, it is known that: $X_3 = B$, and the dynamic angle of repose when the belt speed is V is γ.

According to the properties of the parabola, the following formula can be listed:

$$F'(0) = \tan(\gamma), \tag{1}$$

$$F'(d) = \tan(\pi - \gamma), \tag{2}$$

$$F\left(-\frac{b}{2a}\right) = h. \tag{3}$$

Solving the system of equations mentioned above:

$$a = -\frac{\tan(\gamma)}{d},$$

$$b = \tan(\gamma),$$

$$c = h + 0.75 * B * \tan(\gamma).$$

That is:

$$F(X) = -\frac{\tan(\gamma)}{d} X^2 + \tan(\gamma) X + h + 0.75B\tan(\gamma). \quad (4)$$

The discharge amount of the primary unloader is obtained by integration as:

$$Q_1 = \rho V \left[\frac{\tan(\gamma)}{6d} \tan^3(\theta_1) + \frac{\tan(\gamma)}{2} \tan^2(\theta_1) + h\tan(\theta_1) + 0.75B\tan(\gamma)\tan(\theta_1) \right]. \quad (5)$$

After the primary unloader has completed unloading, the remaining material on the belt will collapse and accumulate again. When the contour trajectory corresponding to the horizontal coordinate X_2 of the opening angle of the secondary unloader has not collapsed, one can first calculate the discharge amount Q_3 of the tertiary unloader, and finally calculate Q_2:

$$Q_2 = Q - Q_1 - Q_3. \quad (6)$$

When the contour trajectory corresponding to the horizontal coordinate X_2 of the opening angle of the secondary unloader collapses, it is necessary to use visual detection methods to detect the corresponding parameters of the material accumulation contour (maximum accumulation height and the limit coordinate X_2' on the X-axis near the unloading mouth). Based on the monitoring data, fit the accumulation contour function after the collapse.

$$F_2(X) = -\frac{\tan(\gamma)}{d} (X + X_0)^2 + \tan(\gamma) * (X + X_0) + h + 0.75 * B * \tan(\gamma) + Y_0. \quad (7)$$

Given the horizontal coordinate X_2 corresponding to the opening angle of the secondary unloader, the discharge amount Q_2 of the secondary unloader is:

$$Q_2 = \rho * V * \int_{X_2'}^{X_2} F_2(X) dX. \quad (8)$$

At the same time, the discharge amount of the tertiary unloader is:

$$Q_3 = Q - Q_1 - Q_2. \quad (9)$$

The material accumulation contour function after the aforementioned secondary collapse is measured at the corresponding positions using detection methods (Wei 2023), and the corresponding X_0 and Y_0 are solved based on the monitoring points, which are then substituted into the discharge model for solution.

2.3. FITTING THE MATERIAL ACCUMULATION CROSS-SECTION CONTOUR WITH A PIECEWISE FUNCTION

When the feeding device opening is large, the material will no longer accumulate in a completely free-stacking form. It will show a smooth change in the middle section and accumulate at both ends according to the dynamic angle of repose, as shown in the figure below.

At this point, a piecewise function is used to describe the material accumulation contour according to the form of material accumulation.

Given the belt width *B*, the plate length *L*, and the angle of the unloader opening as θ (with the maximum value $\theta_{\max} = \arcsin\frac{B}{L}$, according to the transportation form, the unloading plate is opened to a certain angle, and the material within the opening angle is unloaded along the guide plate from the opening.

Through simulation and experimental detection of actual working conditions, the shape of the material accumulation on the belt is shown in Fig. 3. The contour is fitted using the piecewise function $f(X)$:

$$f(x) = \begin{cases} F(x) & 0 < x < \dfrac{(B-d)}{2} \ \ or \ \ \dfrac{(B+d)}{2} < x < B \\ m & \dfrac{(B-d)}{2} < x < \dfrac{(B+d)}{2} \end{cases}. \tag{10}$$

The accumulation pattern of the material on the belt under actual working conditions was detected through simulation and experimental analysis, as depicted in Fig. 3. A piecewise function, denoted as *f*(*X*), was utilized to fit this profile. Here, "*m*" represents the feeding coefficient, a constant indicative of the feeder opening size, which within the model signifies the width at which the material is uniformly accumulated on the belt. The magnitude of "*m*" is correlated with the feeding velocity. Based on the fitting function, the unloading rates at the discharge port can be calculated as follows:

$$Q_1' = \rho * V * \int_0^{X_1'} f(X)dX. \tag{11}$$

From the fitted function, it is inferred that the discharge rate of the tertiary unloader is unaffected when the aperture angle of the secondary unloader is less than $\frac{(B+d)}{2}$. Consequently, the discharge rate Q_3' of the tertiary unloader is calculated first.

$$Q_3' = \rho * V * \int_{X_2'}^{B} f(X)dX. \tag{12}$$

The secondary unloading amount Q_2':

$$Q_2' = Q - Q_1' - Q_3'. \tag{13}$$

From the unloading expression, it can be inferred that when the dimension of the feed opening along the width direction of the belt is large, the material will be evenly spread in the middle *d* on the belt. At this point, the unloading of the tertiary unloader is affected only when the coordinate corresponding to the opening angle of the secondary unloader, $\frac{(B+d)}{2} < X$, influences the accumulation contour of the corresponding material. At this time, the secondary unloader is almost fully open. Therefore, in this fitting scenario, the changes in the unloading amount of the tertiary unloader caused by the collapse and re-accumulation of materials due to an excessively large opening angle of the secondary unloader are not considered.

3. EXPERIMENTAL PLATFORM SETUP

3.1. OVERALL DESIGN SCHEME

The coal-rejecting machine is mainly used for conveying backfilling materials during mine pit backfilling. It is generally hoisted on a hydraulic support. Since the entire machine is hoisted on the hydraulic support, it cannot ensure that every section of the conveyor belt moves simultaneously during movement, and the ground is uneven. Therefore, it is necessary for the coal-rejecting machine to achieve a small angle deflection between every two sections. When designing the experimental platform, the deflection angle between each section is set to be horizontal ±1.5° and vertical ±3° after considering the precision. The thickness of the belt coal-rejecting machine should not exceed the commonly used bottom-discharge scraper conveyor, and it should achieve a certain initial speed for the material to be thrown out. The experimental test platform for the belt coal-rejecting machine is shown in Fig. 5. The platform mainly includes a feeding device, tension adjustment and deflection device, unloading device, material collection device, and measurement control system.

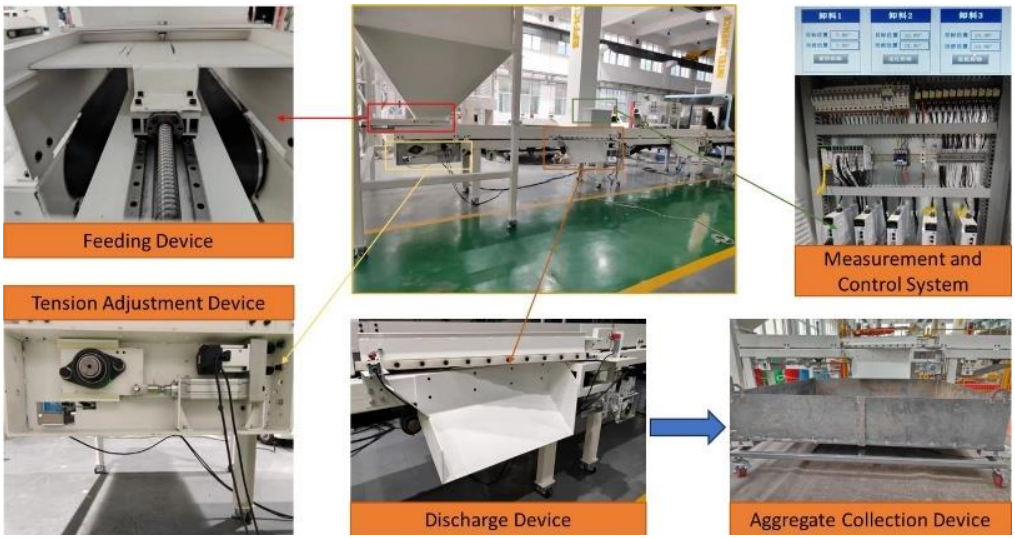

Fig. 5. Belt coal-rejecting machine experimental test platform

In response to the design requirements, deflection is achieved in each section by connecting with a dumbbell pin, allowing for deflection in four directions: up, down, left, and right, making the platform design more realistic. The entire machine is driven by a variable frequency speed-regulated electromagnetic brake three-phase asynchronous motor, model YVF2EJ-132S-4, with a power of 5.5 kW. The variable frequency speed regulation controls the rotation speed to adjust the belt speed, enabling analysis of unloading performance at different belt speeds and a wide range of unloading.

3.2. KEY STRUCTURAL DESIGN

3.2.1. FEEDING DEVICE

The feeding device must meet the experimental requirements. It mainly consists of a buffer hopper and an electric sliding table. The electric sliding table is controlled by a servo motor to move the material stopper back and forth. The servo motor selected is model SV-X2MA040A-B2CA. The feeding device is shown in Fig. 6.

The design of the buffer hopper's angle of inclination is one of the main factors determining the feeding speed, and an angle of 20° to 35° is more conducive to feeding (Wang et al. 2024). Based on actual working conditions, this experimental platform selects a buffer hopper angle of 30° (with a 30° angle, when the material stopper is fully open at a belt speed of 2 m/s, the maximum material flow rate can reach 100 kg/s). Under a certain hopper angle, the flow of coal and gangue particles from the buffer hopper to the electric sliding table position depends on the size of the opening formed by

the electric sliding table and the buffer hopper. The electric sliding table is controlled by a servo motor, which can freely adjust the reciprocating motion of the electric sliding table, thereby indirectly adjusting the size of the material flow.

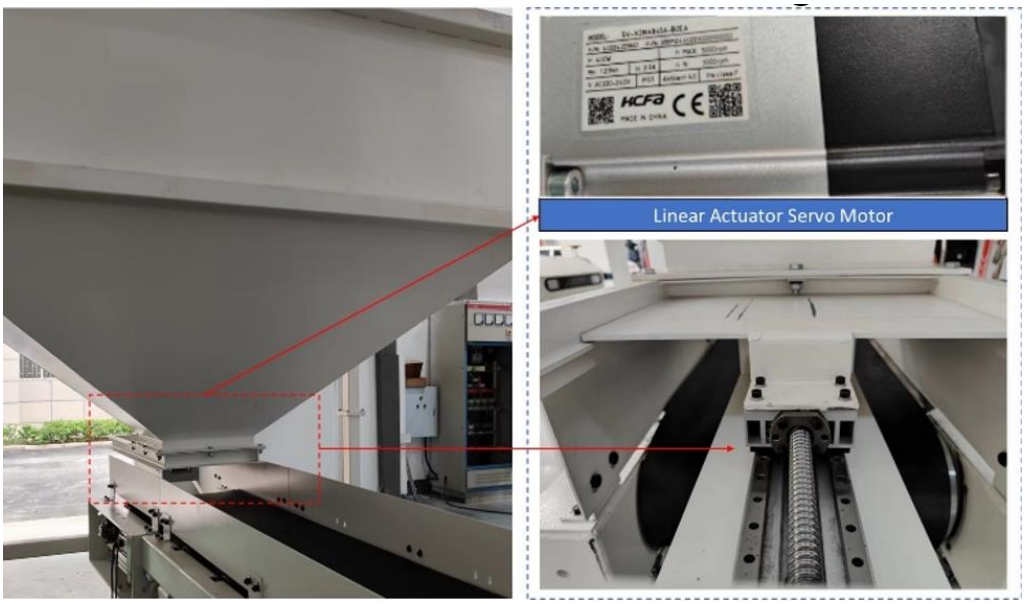

Fig. 6. Feeding device

3.2.2. TENSIONING AND ALIGNMENT ADJUSTMENT DEVICE

The tensioning mechanism in a belt conveyor system is a crucial component that ensures the stable operation of the belt. This mechanism consists of two symmetrically assembled servo cylinders that work in coordination through an accurate control system to achieve precise adjustment of the belt tension. The design of the servo cylinder allows for the adjustment of the belt's tension by changing its extension length, thereby adapting to different loads and operating conditions. The alignment adjustment mechanism is another important function of the tensioning device. By independently controlling the extension and retraction of the cylinders on both sides, operators can make lateral adjustments to the belt, ensuring accurate guidance of the material during the conveying process. This type of adjustment not only increases the flexibility of the system but also significantly reduces maintenance costs and potential downtime due to belt misalignment.

The tensioning and alignment adjustment device is composed of two symmetrically distributed servo cylinders and two travel switches. The servo cylinders are made up of a rod-style cylinder and a servo motor, as shown in Fig. 7.

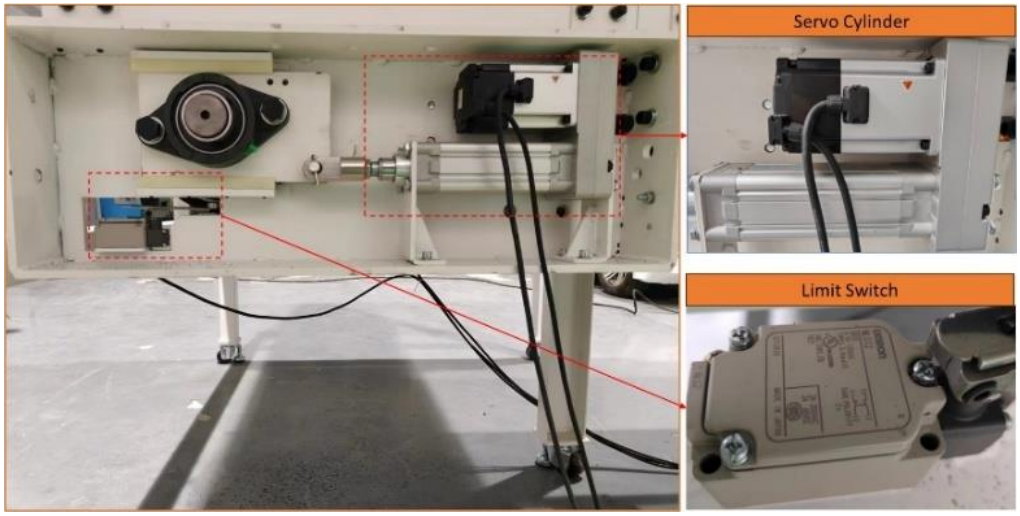

Fig. 7.Tensioning and alignment adjustment device

During the operation of this experimental platform, due to the simulation of actual working conditions with a 1.5° deflection design for each section of the platform, and the sliding contact with the ground at the bottom, the belt will experience significant deflection which severely affects its service life and the stable operation of the platform. The servo cylinder needs to adjust the deflection to ensure the stable operation of the platform, thereby obtaining a stable result in the experiment.

3.2.3. UNLOADING DEVICE

The unloading device is the core component of the coal-rejecting machine, and its main function is to adjust the opening angle of the plow-type board so that the material is thrown out along the board. The belt speed, opening angle, and board type are all factors that affect the transverse throwing speed of the material. To study the influencing factors of the throwing performance, the experimental platform is designed with a detachable unloading device, which can measure the throwing performance through equipment parameters.

The unloading device is mainly divided into three parts, starting from the feeding device direction, it is divided into primary, secondary, and tertiary unloaders. Each level of unloading consists of a single-sided plow-type unloading device, two limit devices, one servo motor and reducer, and one guide plate. According to the design calculation, a servo motor model SV-X2MA040A-B2CA with a power of 400 W and a reducer model DRV(63-90)-1200-AS2-ST60-14-5 are selected for control. Limit devices 1 and 2 correspond to the minimum and maximum opening angles of the single-sided plow-type unloading device, respectively. The unloading device is shown in Fig. 8.

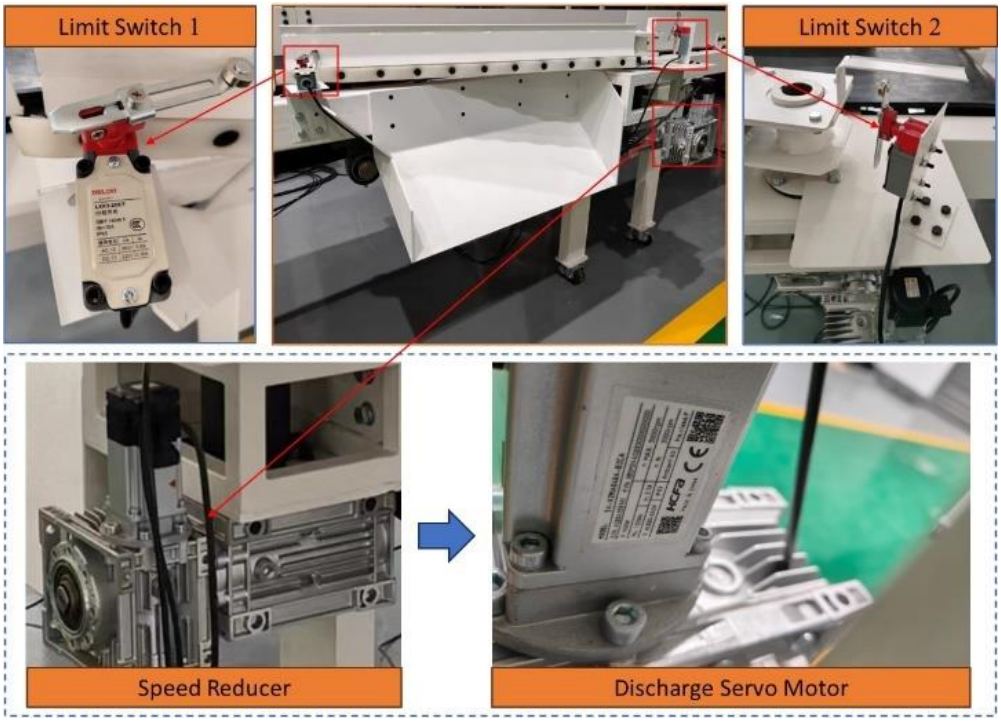

Fig. 8. Unloading device

Simulations have revealed that when the belt speed is 6m/s and the output is 400 t/h, no clogging will occur when the angle between the single-sided plow-type unloading device and the conveyor belt is less than 40° (Yao and Gu 2023), hence the opening angle is designed to be 0°~40°. Material falls from the feeding device and, under the action of the conveying device, flows towards the single-sided plow-type unloading device at a certain speed. Subsequently, after the material forms a stable motion and
a specific accumulation shape, the opening angle of the single-sided plow-type unloading device is controlled to make the material follow a specific trajectory, thereby achieving precise unloading.

4. EXPERIMENTAL VERIFICATION

4.1. EXPERIMENTAL PLAN

Based on the mathematical model established in the previous text, it is found that the accumulation shape of the material is a key factor affecting the unloading amount. To

verify the correctness of the unloading mathematical model, this paper selects the unloading form of the tertiary unloader for the experiment (at this time, the collapse of the material after unloading by the primary unloader does not affect the unloading amount of the tertiary unloader (Wu 2022)). The belt width B is 500 mm, and the belt speed V is 2 m/s, with the corresponding transport capacity Q of 35 kg/s. The unloading device opening range is 0–40°. Stones are used as the material, with a dynamic accumulation angle γ of 35° at a belt speed V of 2 m/s, h is taken as 0.25 m, and ρ is taken as 1200 kg/m³.

The angle at which the collapse of the material after unloading by the primary unloader does not affect the unloading amount of the tertiary unloader is taken as the working condition angle for verification.

(1) Fit the material accumulation contour with a parabolic curve: When the material is in a state of complete free stacking.

$$Q_1 = \rho V\left[\frac{\tan(\gamma)}{6d}\tan^3(\theta_1) + \frac{\tan(\gamma)}{2}\tan^2(\theta_1) + h\tan(\theta_1) + 0.75d\tan(\gamma)\tan(\theta_1)\right], \quad (14)$$

$$Q_3 = \rho * V * \int_{X_2}^{X_3} F(X)dX, \quad (15)$$

$$Q_2 = Q - Q_1 - Q_3. \quad (16)$$

Let $Q_1 = Q_2 = Q_3$ to obtain an approximate solution:

$$\begin{cases} \theta_1 = 14.7° \\ \theta_2 = 22.8°. \\ \theta_3 = 40.0° \end{cases}$$

(2) When the material is not completely stacked (with the feed opening width taken as 0.3 m, and the feeding coefficient d detected to be 0.36, m = 0.22, make $\frac{(B-d)}{2} = d_1$, $\frac{(B+d)}{2} = d_2$.

$$Q_1 = \rho * V * \int_{0}^{X_1} f(X)dX, \quad (17)$$

$$Q_2 = \rho * V * \int_{d_1}^{X_2} f(X)dX, \quad (18)$$

$$Q_3 = \rho * V * \int_{X_2}^{X_3} F(X)dX. \tag{19}$$

Let $Q_1 = Q_2 = Q_3$ to obtain an approximate solution:

$$\begin{cases} \theta_1 = 14.1° \\ \theta_2 = 23.9°. \\ \theta_3 = 40.0° \end{cases}$$

4.2. SIMULATION EXPERIMENT

(1) Since it is difficult for the material to achieve complete free stacking during the actual unloading process, EDM simulation methods are used. Material is continuously conveyed in an approximate complete free stacking form, and the opening angles of the

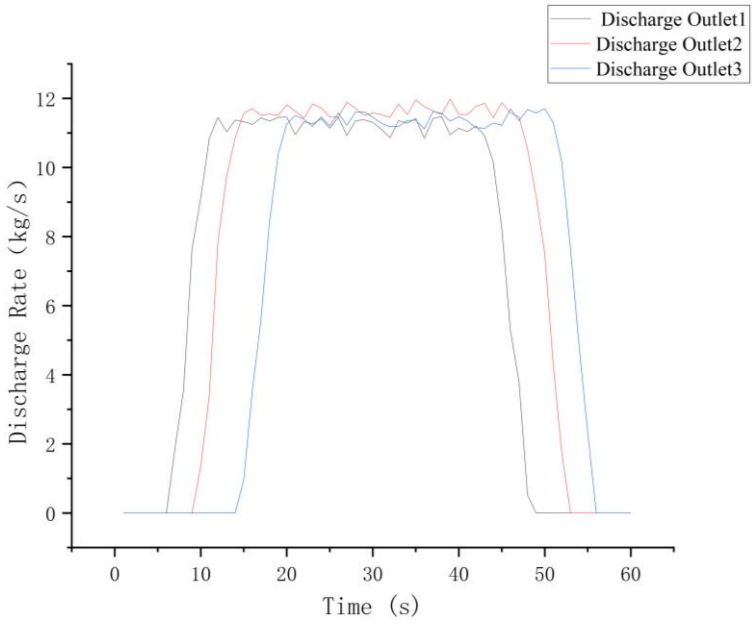

Fig. 9. Natural accumulation simulation unloading speed

three unloading devices are adjusted according to the complete free stacking unloading model for simulation. The total time is 12 seconds, and the change curves of the unloading speeds corresponding to the three unloading mouths are shown in Fig. 9.

From the simulation results, it can be seen that when close to complete free stacking, the average unloading speeds of each unloading mouth are 11.13 kg/s, 11.86 kg/s, and 11.29 kg/s, respectively. The unloading model is in uniform unloading when the

unloading mouth is opened to this angle. The total transport capacity is 35 kg/s, and the average unloading amount for each unloading mouth is 11.67 kg/s. Compared with the simulation results, the maximum error of the three unloading mouths is 2.7%.

The unloading speeds of each unloading mouth are shown in Fig. 10 according to the simulation of the angles fitted by the piecewise function to the contour.

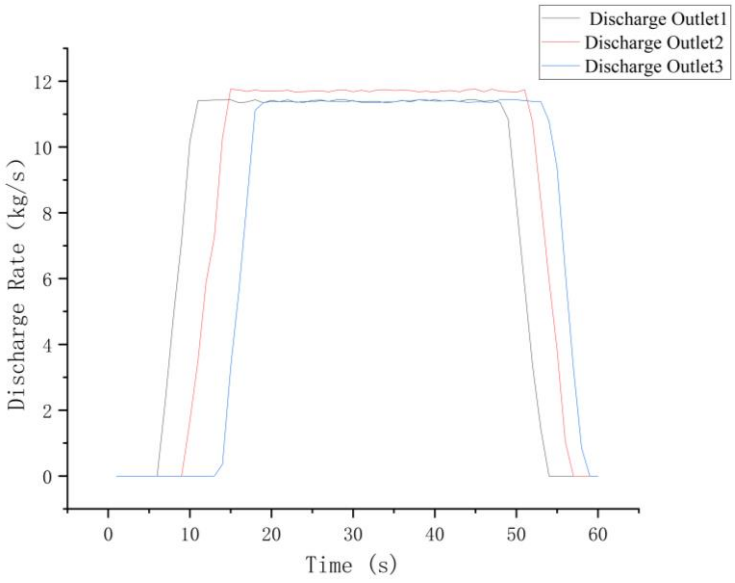

Fig. 10. Piecewise function unloading simulation

From the simulation results, it is known that when the material is close to complete free stacking, the unloading speeds of the three unloading mouths are 11.35 kg/s, 11.78 kg/s, and 11.08 kg/s, respectively. The maximum error of this model compared to equal unloading is 3.5%.

(2) Material throwing experiment simulation

In actual operation, the coal-rejecting machine cannot achieve complete free stacking of materials on the belt due to practical working conditions. To conform to the actual conditions, an experiment is conducted using a feed opening of 300 × 300 mm in size. The opening angles of the unloading devices are set to the opening angles calculated for uniform unloading in both unloading models.

Multiple experiments are conducted with two combinations of opening angles, and the average unloading speeds are recorded. The comparison between the experimental and simulation results is shown in the following Table 1.

From the above table, it can be seen that during actual unloading, due to processing and installation errors, the material leakage is approximately 8.46%. The errors in unloading quantities at each level compared to the natural accumulation simulation

and experiment are 6.91%, 5.99%, and 9.74%, respectively; the errors in unloading quantities at each level compared to the piecewise fitting simulation and actual unloading are 8.72%, 5.35%, and 8.03%, respectively.

Table 1. Comparison of experimental and simulated unloading quantities

Unloading mouth	Experimental unloading speed	Natural accumulation	Piecewise fitting
1	10.36	11.13	11.35
2	11.15	11.86	11.78
3	10.19	11.29	11.08

4.3. EXPERIMENTAL RESULTS ANALYSIS

By comparing the simulation and experimental results with the model, it is evident that the errors of both models do not exceed 10%. Under the current feed opening conditions, the unloading model fitted with the piecewise function has a smaller error when compared to the actual unloading volume. This is because when the operating conditions are close to complete free stacking, the material will undergo a secondary collapse after being unloaded by the primary unloading device. If the opening angle is still set according to the original fitting function, the unloading volume of the tertiary unloading device will be underestimated, resulting in a deviation based on the extent of the collapse. When the material accumulation shape has a certain degree of uniform spreading in the middle, the experimental results indicate that the impact of collapse caused by changes in the opening angle will be reduced.

5. CONCLUSION

Two unloading models for belt-type gob Backfilling Slingers, Model A and Model B, have been established. Model A is suitable for situations where the material accumulation form is close to complete free stacking; Model B is suitable for situations where the material accumulation shape on the belt includes a certain range that is close to a flat laying section.

Through comparison of simulation and material throwing experiments, Model A has an error of no more than 3% when the material is close to complete free stacking and the collapse of the material after the first unloading does not affect the opening angle of the second unloading. When the setting value of the tertiary unloading volume is greater than one-third of the total transport volume, the error of this unloading model will exceed 10%. The main error occurs because after the first unloading, the

material collapses after being transported for the length of one section of the belt machine. To reduce the error caused by the collapse, it is necessary to install corresponding sensors to detect the parameters of the re-accumulated material contour, and then re-fit the contour function according to the model to obtain the opening angle of the secondary unloading device.

Model B was found through experimental validation using the experimental platform: when the belt width is 0.5 m and the feed opening is 0.3×0.3m, the actual unloading volume has an error of no more than 5% with the model. However, since the material does not achieve complete free stacking, the uniformity of the material distribution on the belt increases, minimizing the impact of the material collapse after the first unloading on the subsequent unloading volume. When the setting value of the tertiary unloading volume is close to half of the total transport volume, the error will not exceed 6.5%.

Comparing the two unloading models, Model A is suitable for occasions that require precise unloading, but it is necessary to install sensors in each set of unloading devices to detect the parameters of the collapsed material accumulation; Model B requires the calculation of the feed coefficient of the feed opening, and does not need to consider the error caused by the material collapse. It is suitable for working environments where it is not suitable to install sensors. By controlling the feed coefficient, the error can be controlled within 5%.

REFERENCES

CLEARY P.W., 2013, *Particulate Mixing in a Plough Share Mixer Using DEM with Realistic Shaped Particles*, Powder Technology, 248, 103–120.

CUI X.R., ZHAI X.P., Zhou B.J. et al., 2025, *Spatial Distribution Characteristics and Graded Utilization Path of Coal Gangue in China*, Environmental Science, 46 (4), 2281–2291, https://doi.org/10.13227/j.hjkx.202401269

HUANG Y.L., 2012, *Ground Control Theory and Application of Solid Dense Backfill in Coal Mines*, PhD diss., China University of Mining and Technology.

MINGLIANG Y., NING Y., and ZHENGWEI Z., 2022, *Research on Structure Optimization of Plow Discharger of Belt Conveyor Based on DEM*, Forest Chemicals Review, 10–33.

WANG Q., YUE Q., DOU Z.H. et al., 2024, *Influence of Hopper Angle on Pellet Flow and Distribution in Gas-Based Shaft Furnace During Charging Process*, Journal of Materials and Metallurgy, 23 (2), 136–144, https://doi.org/10.14186/j.cnki.1671-6620.2024.02.004

WANG XUEWEN et al., 2018, *The Transporting Efficiency and Mechanical Behavior Analysis of Scraper Conveyor*. Proceedings of the Institution of Mechanical Engineers, Part C, Journal of Mechanical Engineering Science, 232 (18), 3315–3324, https://doi.org/10.1177/0954406217734002

WEI F., 2023, *Application of Real-Time Detection Technology for Coal Gangue in Belt Conveyors*, Mining Equipment, (10), 34–35.

WU Y.S., 2022, *Investigation on Granular Collapsing Flow Driven by Gravity and Its Interaction with Different Media*, PhD diss., Lanzhou University, https://doi.org/10.27204/d.cnki.glzhu.2022.003638

WU Y.Y., LIU C.Y., ZHANG P. et al., 2024, *Principle of Fully Mechanized Gangue-Throwing Filling Technology and the Sand-Throwing Test*, Coal Engineering, 56 (5), 69–74.

YANG N., 2022, *Research on Structure Optimization of Plow Discharger of Belt Conveyor Based on DEM*, Master's thesis, Taiyuan University of Science and Technology. https://doi.org/10.27721/d.cnki.gyzjc.2022.000554

YAO Y. and GU X., 2023, *Research on Discharge Plate of Plough Tripper Based on Discrete Element*, Journal of Physics: Conference Series, 2665 (1), 012008, IOP Publishing, https://doi.org/10.1088/1742-6596/2665/1/012008

YIN R., Zhang D.X., and NI Q., 2024, *Research on the Transportation Model and Coal Quantity Calculation Algorithm of Scraper Conveyor Based on Array*, Journal of Mine Automation, 1–7, https://doi.org/10.13272/j.issn.1671-251x.2024070052 [Accessed September 6, 2024].

ZHAO M.J., 2020, *Study on Calculation Method of Air Cushion Pressure Distribution of Air Cushion Belt Conveyor*, PhD diss., Northeastern University, https://doi.org/10.27007/d.cnki.gdbeu.2020.000602